

## Electron tunneling spectroscopy study of amorphous films of the gate dielectric candidates $\text{LaAlO}_3$ and $\text{LaScO}_3$

M. Wang, W. He, and T. P. Ma<sup>a)</sup>

*Department of Electrical Engineering, Yale University, New Haven, Connecticut 06520*

L. F. Edge and D. G. Schlom

*Department of Materials Science and Engineering, Pennsylvania State University, University Park, Pennsylvania 16802-5005*

(Received 20 November 2006; accepted 4 January 2007; published online 30 January 2007)

Electron tunneling spectroscopy (ETS) was used to study amorphous  $\text{LaAlO}_3$  and  $\text{LaScO}_3$  thin film gate dielectrics for silicon metal-oxide-semiconductor structure. These gate dielectrics were prepared by molecular-beam deposition on (100) Si substrates. The authors have obtained vibrational modes for amorphous  $\text{LaAlO}_3$  and  $\text{LaScO}_3$  thin films from the ETS spectra, which provide information about the chemical bonding in these films and the interface with silicon. Traps and defects in amorphous  $\text{LaAlO}_3$  thin films are revealed in the ETS spectra, and their physical locations and energy levels are identified. © 2007 American Institute of Physics.

[DOI: 10.1063/1.2437128]

Amorphous  $\text{LaAlO}_3$  and  $\text{LaScO}_3$  are being investigated as promising high- $\kappa$  gate dielectrics due to their high dielectric constants (16–27 for amorphous  $\text{LaAlO}_3$  and 22 for amorphous  $\text{LaScO}_3$ ),<sup>1–5</sup> high optical band gaps (6.2 eV for amorphous  $\text{LaAlO}_3$  and 5.72 eV for amorphous  $\text{LaScO}_3$ ),<sup>6–8</sup> and abrupt interfaces when grown on silicon.<sup>9,10</sup> Many issues, however, including high leakage current densities, high densities of bulk traps, and poor interface properties, remain to be resolved. It is very important to be able to probe the underlying mechanisms behind these challenging issues. Electron tunneling spectroscopy (ETS), which is obtained by taking the second derivative of the current-voltage ( $I$ - $V$ ) characteristic of a tunnel barrier, probes the metal-oxide-semiconductor (MOS) structure by detecting interactions between the tunneling electrons, lattice vibrations (phonons), impurities, and defects in the gate dielectric.<sup>11–13</sup>

In this study, we applied ETS as a characterization tool to identify the vibrational modes of amorphous  $\text{LaAlO}_3$  and  $\text{LaScO}_3$  gate dielectrics, and we used this technique to detect the traps in amorphous  $\text{LaAlO}_3$  thin films.

The MOS capacitors in this study were fabricated on  $n$  type, (100) silicon substrates. Degenerate silicon wafers ( $>10^{19}/\text{cm}^3$ ) were used to ensure conduction during the ETS measurements, which were performed in liquid He at 4.2 K. The amorphous  $\text{LaAlO}_3$  and  $\text{LaScO}_3$  layers ( $\sim 110$  Å thick) were grown by molecular-beam deposition at room temperature.<sup>5,9,10,14</sup> The films were deposited at a background partial pressure of oxygen of  $6 \times 10^{-7}$  Torr. A 3000 Å thick blanket Al top electrode was deposited *in situ*, without breaking vacuum, immediately after the oxide deposition. The Al electrode was patterned using photolithography and then wet etched. The area of each MOS capacitor was 1.3 mm<sup>2</sup>.

Figure 1 shows the forward- and reverse-biased ETS spectra of an amorphous  $\text{LaAlO}_3$  MOS capacitor. The spectra are featureless between 130 and 180 mV, where  $\text{SiO}_2$  peaks would be located.<sup>15</sup> This indicates that there is no  $\text{SiO}_2$  at the interface between  $\text{LaAlO}_3$  and Si, in agreement with

the results from other characterization techniques on similar films.<sup>9,14</sup>

Figure 2 shows the vibrational modes of amorphous  $\text{LaAlO}_3$  thin films obtained by deconvolution. The vibrational modes of the amorphous  $\text{LaAlO}_3$  thin films extracted from the ETS spectra are listed in Table I. Most of the amorphous  $\text{LaAlO}_3$  modes coincide with phonons in crystalline  $\text{LaAlO}_3$  obtained from Raman, infrared, and theoretical calculations.<sup>16–19</sup> The feature at around 34 meV arises from ionized donors in the silicon substrate.<sup>15</sup> The peaks at 19, 44, 51, and 61 meV may also come from the silicon substrate.<sup>15</sup> We should note that, like other high- $\kappa$  materials, most of the modes from amorphous  $\text{LaAlO}_3$  are located from 15 to 95 meV. These soft modes may have a strong effect on scattering the electrons in the channel and therefore could degrade the electron mobility.<sup>20</sup>

The energy levels and the physical locations of traps in the gate dielectric can be estimated from trap-assisted tunneling in a MOS capacitor by the voltage bias polarity dependence of trap features in the spectrum.<sup>21</sup> The voltages where the trap-assisted tunneling features occur in the forward- and reverse-biased spectra depend on the energy levels and the physical locations of traps. It can be shown

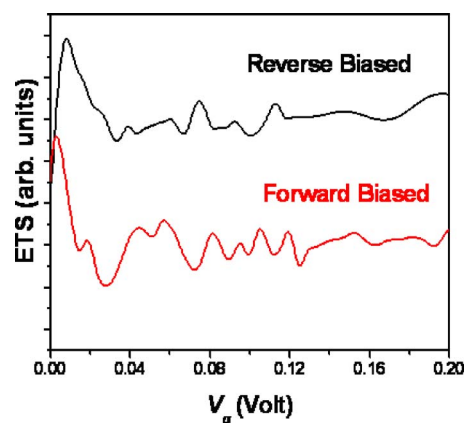


FIG. 1. Forward- and reverse-biased ETS spectra from an Al/amorphous  $\text{LaAlO}_3$ /Si MOS capacitor.

<sup>a)</sup>Electronic mail: t.ma@yale.edu

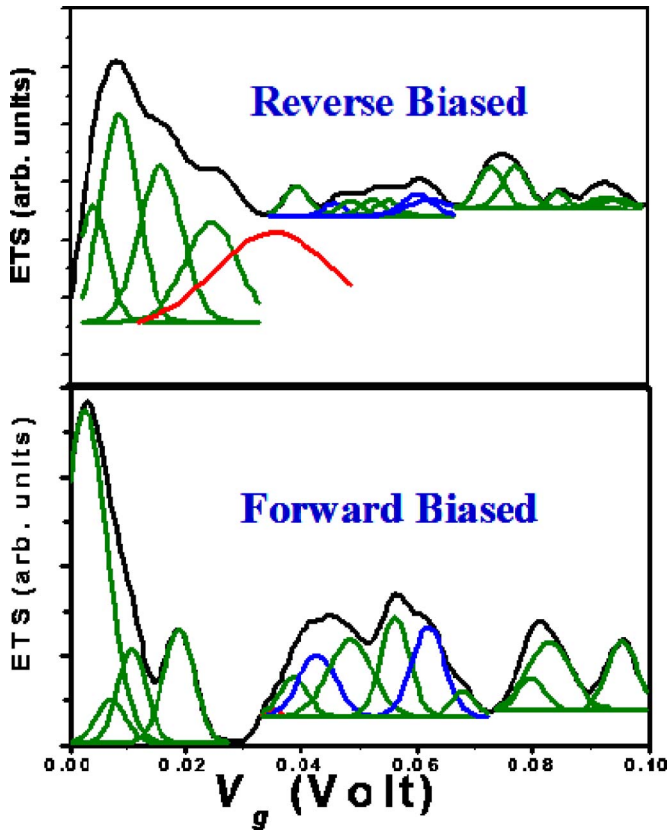


FIG. 2. Vibrational modes from an amorphous LaAlO<sub>3</sub> thin film measured by ETS.

that the trap energy level  $V_t$ , defined by its energy above the Fermi level of the electrodes at zero bias, can be expressed as

$$V_t = V_r V_f / (V_r + V_f), \quad (1)$$

where  $V_f$  and  $V_r$  are the voltages of the forward- and reverse-bias trap features, respectively. We define  $V_f$  as the forward bias (gate positive) where the Fermi level of the negatively biased electrode (substrate) reaches the energy level of the trap.

The physical location of the trap can be expressed by

$$d_t = d_0 V_f / (V_f + V_r), \quad (2)$$

where  $d_0 = \int_0^{x_0} 1/\epsilon(x) dx$  and  $d_t = \int_0^{x_t} 1/\epsilon(x) dx$ .  $x_0$  is the total physical thickness of the dielectric,  $x_t$  is the distance of the trap from the gate/dielectric interface,  $d_0$  is the effective electrical thickness of the dielectric, and  $d_t$  is the effective electrical distance of the trap from the gate electrode. Note that the expressions shown above take into account the general case where the dielectric constant varies in the direction perpendicular to the surface (the  $x$  direction), i.e., a nonuniform dielectric constant:  $\epsilon = \epsilon(x)$ .

Figure 3 shows the forward- and reverse-biased spectra of an amorphous LaAlO<sub>3</sub> thin film in which prominent trap-

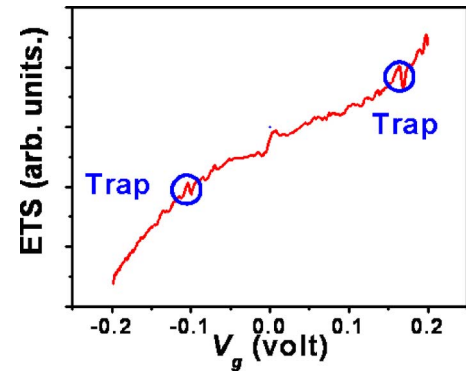


FIG. 3. Trap-assisted tunneling features revealed by ETS in an amorphous LaAlO<sub>3</sub> thin film. The traps have an energy level 62–64 meV above the Fermi level at zero bias and occur 28–30 Å from the amorphous LaAlO<sub>3</sub>/Si interface.

assisted tunneling features are revealed. Based on the fact that the forward- and reverse-bias trap features reproducibly occur at the same location in the voltage sweep from reverse to forward bias, we assume the trap features in Fig. 3 are caused by the same traps. By the expression outlined above, we are able to estimate the trap energy level to be  $63 \pm 1$  meV above the Fermi level at zero bias. The location of the trap is  $29 \pm 1$  Å from the gate dielectric-substrate interface. Two major aspects of the above plots are (1) the prominent trap features, which suggest a significant defect concentration in the bulk that assist in electron tunneling and increase the leakage, and (2) the trap feature revealed in the forward-biased spectrum, which is stronger than in the reverse-biased spectrum. This is caused by the asymmetry of the tunneling barrier, which gives rise to a higher tunneling probability in the forward direction.

Figure 4 illustrates the forward- and reverse-biased ETS spectra from an amorphous LaScO<sub>3</sub> thin film. No features were detected from 130 to 180 meV, where SiO<sub>2</sub> peaks would be located, indicating the absence of SiO<sub>2</sub> at the interface between LaScO<sub>3</sub> and silicon. This is in agreement with the results of other measurement techniques on similar samples.<sup>10</sup> The vibrational modes for amorphous LaScO<sub>3</sub> are listed in Table II. In the reverse-biased spectrum, the silicon phonon modes show up at 17, 46, 55, and 62 meV.<sup>15</sup> Significant differences exist between the forward-biased and reverse-biased spectra, primarily due to the forward-biased signal coupling much more strongly with the dielectric/top-electrode interface, while the reverse biased one tends to couple much more strongly with the dielectric/substrate interface.<sup>22</sup>

In summary, we have applied ETS to study MOS capacitors with amorphous LaAlO<sub>3</sub> and LaScO<sub>3</sub> gate dielectrics on silicon substrates. Using ETS, we obtained the vibrational modes and trap information (including trap energies and physical locations) for amorphous LaAlO<sub>3</sub> and LaScO<sub>3</sub> from their ETS spectra. The ETS spectra provide information

TABLE I. Phonon energies of amorphous LaAlO<sub>3</sub> obtained from ETS spectra (unit: meV).

Forward bias	19 <sup>a</sup>	24	30	35 <sup>b</sup>	37	40	44 <sup>a</sup>	48	50 <sup>a</sup>	56	62 <sup>a</sup>	68	79	86	91
Reverse bias	16	19 <sup>a</sup>	29	34 <sup>b</sup>	37	39	46 <sup>b</sup>	48	52 <sup>a</sup>	55	61 <sup>a</sup>	66	73	79	92

<sup>a</sup>Peaks which may come from the Si substrate.

<sup>b</sup>Feature which may arise from ionized donors in the silicon substrate.

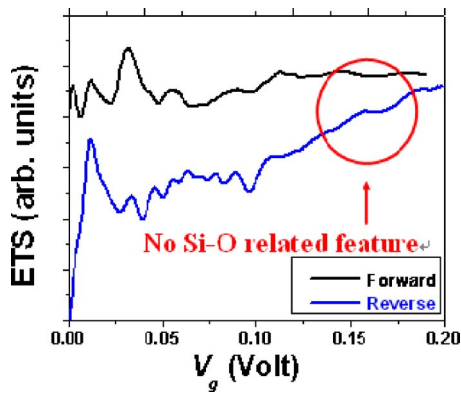


FIG. 4. Forward- and reverse-biased ETS spectrum from an Al/amorphous LaScO<sub>3</sub>/Si MOS capacitor. The featureless region circled indicates the absence of SiO<sub>2</sub> at the LaScO<sub>3</sub>/Si interface.

about the interfaces and chemical bonding structures in these films.

The authors gratefully acknowledge the financial support of the Semiconductor Research Corporation (SRC) and SEMATECH through the SRC/SEMATECH FEP Center. One of the authors (L.F.E.) gratefully acknowledges an AMD/SRC fellowship, and (M.W.) gratefully acknowledges partial support from the National Science Foundation under Contract No. MRSEC DMR 0520495.

TABLE II. Phonon energies of amorphous LaScO<sub>3</sub> obtained from ETS spectra (unit: meV).

Forward											
bias	15	25	30	52 <sup>a</sup>		71	78	83	85	89	93
Reverse											
bias	17 <sup>a</sup>	24	46 <sup>a</sup>	55 <sup>a</sup>	62 <sup>a</sup>	71	78			89	

<sup>a</sup>Peaks which may come from the Si substrate.

- <sup>1</sup>B.-E. Park and H. Ishiwara, Appl. Phys. Lett. **79**, 806 (2001).
- <sup>2</sup>B.-E. Park and H. Ishiwara, Appl. Phys. Lett. **82**, 1197 (2003).
- <sup>3</sup>X.-B. Lu, Z.-G. Liu, Y.-P. Wang, Y. Yang, X.-P. Wang, H.-W. Zhou, and B.-Y. Nguyen, J. Appl. Phys. **94**, 1229 (2003).
- <sup>4</sup>C. Zhao, T. Witters, B. Brijs, H. Bender, O. Richard, M. Caymax, T. Heeg, J. Schubert, V. V. Afanas'ev, A. Stesmans, and D. G. Schlom, Appl. Phys. Lett. **86**, 132903 (2005).
- <sup>5</sup>L. F. Edge, D. G. Schlom, P. Sivasubramani, R. M. Wallace, B. Holländer, and J. Schubert, Appl. Phys. Lett. **88**, 112907 (2006).
- <sup>6</sup>L. F. Edge, D. G. Schlom, S. A. Chambers, E. Cicerella, J. L. Freeouf, B. Holländer, and J. Schubert, Appl. Phys. Lett. **84**, 726 (2004).
- <sup>7</sup>V. V. Afanas'ev, A. Stesmans, L. F. Edge, D. G. Schlom, T. Heeg, and J. Schubert, Appl. Phys. Lett. **88**, 032104 (2006).
- <sup>8</sup>E. Cicerella, J. L. Freeouf, L. F. Edge, D. G. Schlom, T. Heeg, J. Schubert, and S. A. Chambers, J. Vac. Sci. Technol. A **23**, 1676 (2005).
- <sup>9</sup>L. F. Edge, D. G. Schlom, R. T. Brewer, Y. J. Chabal, J. R. Williams, S. A. Chambers, C. Hinkle, G. Lucovsky, Y. Yang, S. Stemmer, M. Copel, B. Holländer, and J. Schubert, Appl. Phys. Lett. **84**, 4629 (2004).
- <sup>10</sup>L. F. Edge, D. G. Schlom, S. Rivillon, Y. J. Chabal, M. P. Agustin, S. Stemmer, T. Lee, M. J. Kim, H. S. Craft, J.-P. Maria, M. E. Hawley, B. Holländer, J. Schubert, and K. Eisenbeiser, Appl. Phys. Lett. **89**, 062902 (2006).
- <sup>11</sup>R. C. Jaklevic and J. Lambe, Phys. Rev. Lett. **17**, 1139 (1966).
- <sup>12</sup>W.-K. Lye, E. Hasegawa, T. P. Ma, R. C. Barker, Y. Hu, J. Kuehne, and D. Frystak, Appl. Phys. Lett. **71**, 2523 (1997).
- <sup>13</sup>W. He and T. P. Ma, Appl. Phys. Lett. **83**, 5461 (2003).
- <sup>14</sup>L. F. Edge, V. Vaithyanathan, D. G. Schlom, R. T. Brewer, S. Rivillon, Y. J. Chabal, M. P. Agustin, Y. Yang, S. Stemmer, H. S. Craft, J.-P. Maria, M. E. Hawley, B. Holländer, J. Schubert, and K. Eisenbeiser, J. Appl. Phys. (submitted).
- <sup>15</sup>W.-K. Lye, Ph.D. Thesis, Yale University, 1998.
- <sup>16</sup>P. Delugas, V. Fiorentini, and A. Filippetti, Phys. Rev. B **71**, 134302 (2005).
- <sup>17</sup>M. V. Abrashev, A. P. Litvinchuk, M. N. Iliev, R. L. Meng, V. N. Popov, V. G. Ivanov, R. A. Chakalov, and C. Thomsen, Phys. Rev. B **59**, 4146 (1999).
- <sup>18</sup>J. F. Scott, Phys. Rev. **183**, 823 (1969).
- <sup>19</sup>P. Calvani, M. Capizzi, F. Donato, P. Dore, S. Lupi, P. Maselli, and C. P. Varsamis, Physica C **181**, 289 (1991).
- <sup>20</sup>M. V. Fischetti, D. A. Neumayer, and E. A. Cartier, J. Appl. Phys. **90**, 4587 (2001).
- <sup>21</sup>M. Wang, W. He, and T. P. Ma, Appl. Phys. Lett. **86**, 192113 (2005).
- <sup>22</sup>C. J. Adkins and W. A. Phillips, J. Phys. C **18**, 1313 (1985).

Applied Physics Letters is copyrighted by the American Institute of Physics (AIP). Redistribution of journal material is subject to the AIP online journal license and/or AIP copyright. For more information, see <http://ojps.aip.org/aplo/aplcr.jsp>